Nano-architectures by covalent assembly of molecular building blocks

LEONHARD GRILL[1]*, MATTHEW DYER[2], LEIF LAFFERENTZ[1], MATS PERSSON[2], MAIKE V. PETERS[3] AND STEFAN HECHT[3]*

[1]Institut für Experimentalphysik, Freie Universität Berlin, Arnimallee 14, 14195 Berlin, Germany
[2]Surface Science Research Centre and Department of Chemistry, University of Liverpool, Liverpool L69 3BX, UK
[3]Institut für Chemie, Humboldt-Universität zu Berlin, Brook-Taylor-Str. 2, 12489 Berlin, Germany
*e-mail: leonhard.grill@physik.fu-berlin.de; sh@chemie.hu-berlin.de

Published online: 28 October 2007; doi:10.1038/nnano.2007.346

The construction of electronic devices from single molecular building blocks, which possess certain functions such as switching or rectifying and are connected by atomic-scale wires on a supporting surface, is an essential goal of molecular electronics[1]. A key challenge is the controlled assembly of molecules into desired architectures by strong, that is, covalent, intermolecular connections[2], enabling efficient electron transport[3] between the molecules and providing high stability[4]. However, no molecular networks on surfaces 'locked' by covalent interactions have been reported so far. Here, we show that such covalently bound molecular nanostructures can be formed on a gold surface upon thermal activation of porphyrin building blocks and their subsequent chemical reaction at predefined connection points. We demonstrate that the topology of these nanostructures can be precisely engineered by controlling the chemical structure of the building blocks. Our results represent a versatile route for future bottom-up construction of sophisticated electronic circuits and devices, based on individual functionalized molecules.

The ability of molecules to form supramolecular structures on surfaces by self-assembly has attracted considerable attention in the last few years[5–9]. The derived patterns, with dimensions almost up to the millimetre range[10], are held together by different non-covalent intermolecular forces such as hydrogen bonding[6,8,11,12], $\pi-\pi$ stacking[10], dipolar[13], van der Waals[14] or metal–ligand[15] interactions. However, no extended molecular networks on surfaces stabilized by interactions that are covalent have been realized yet. In contrast to supramolecular structures, these chemical bonds could facilitate efficient charge transport[3] and high stability[4]. Such large networks are difficult to make by traditional repetitive chemical synthesis, and are not easy to deposit on surfaces while remaining intact. Although it has been shown that the scanning tunnelling microscope (STM) can be used to create covalent bonds between single molecules on a surface[16], this method is not suitable for applications where a large number of molecules need to be connected in a desired architecture.

We have developed a method that overcomes this problem and creates covalently bound nano-architectures, that is, macromolecular structures with controlled shape and size. Our approach is based on small molecular building blocks with reactive side groups (legs) that form permanent chemical bonds at predefined connection points. This concept is illustrated in Fig. 1a, where a chemically stable, central molecular unit, possessing a certain function (that is, an electronic/magnetic/catalytic property), is equipped with several legs. After dissociation of the substituent atoms in the first step by heating, the monomer building blocks are connected with each other through the activated legs, directly on the surface, by thermal diffusion. The ability to design and synthesize molecules with a different number and relative arrangement of predefined connection points allows the construction of various topologies such as dimers, linear chains and two-dimensional arrays.

We present two alternative methods (called methods I and II in the following) for the activation of the molecular building blocks that can be used for the construction of covalently bound nanostructures and lead to similar results. In method I, intact molecules are deposited onto the surface, where they are subsequently activated by dissociation of the substituent atoms upon heating of the sample. In method II, this activation has already occurred in the evaporator, and the activated molecules are subsequently deposited on the surface, kept at room temperature. In both cases, the activated building blocks are covalently connected directly on the surface upon thermal diffusion.

The design of suitable molecules for the formation of such nanostructures requires the incorporation of latent reactive legs that can be activated selectively, without breaking the other bonds. For this purpose, carbon–halogen bonds, exhibiting much smaller binding energies compared with the central framework[16,17], were chosen. After selective thermal dissociation either on the surface (method I) or in the evaporator (method II), the resulting activated (most likely radical) fragments can combine in an addition reaction without producing further byproducts. Considering these requirements, we have chosen a porphyrin with four phenyl legs as a central building block. This molecule is chemically stable and, moreover, mobile on metal surfaces[13,18], which is essential for efficient intermolecular connection. At each leg, bromine was used as the labile substituent atom to be dissociated in a controlled manner. Figure 1b shows the chemical structure of the tetra(4-bromophenyl)porphyrin (Br_4TPP) molecule we used (the Co complex of Br_4TPP has recently been studied in the context of the Kondo effect[19]).

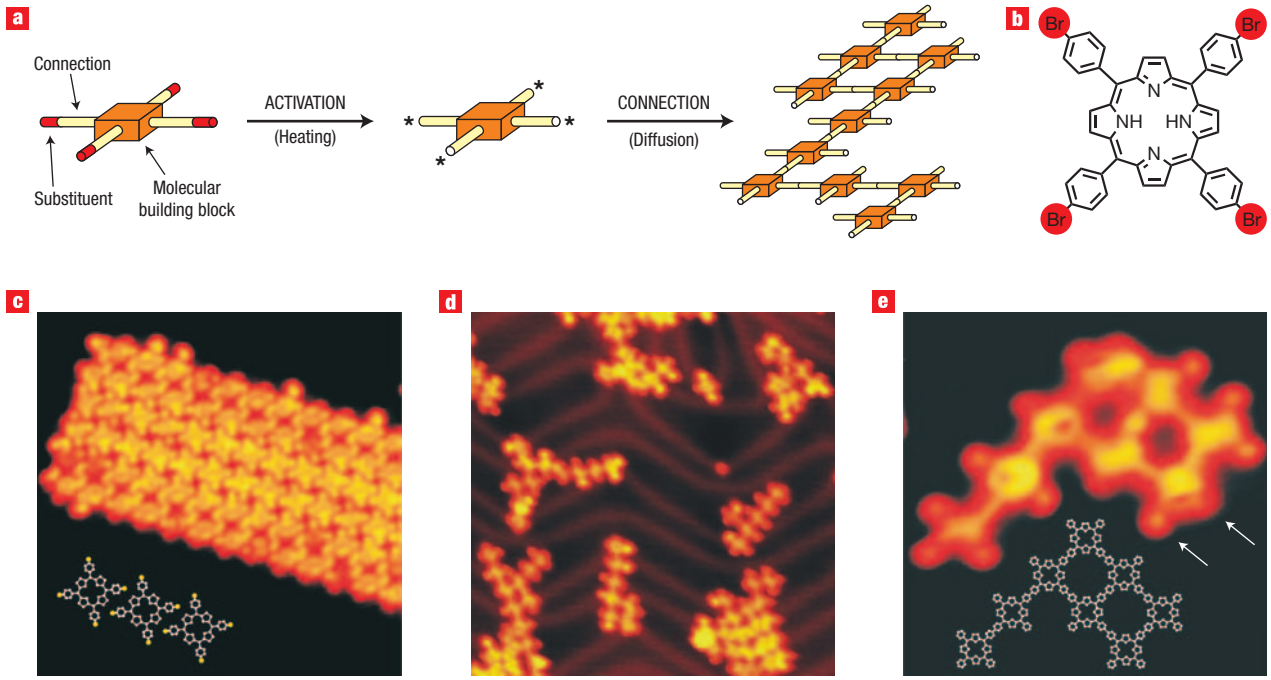

Figure 1 Nano-architectures of covalently bound Br_4TPP molecular networks. a, Concept of the formation of covalently bound networks by connecting activated molecular building blocks. **b**, Chemical structure of the Br_4TPP molecule (substituent Br atoms are highlighted in red). **c**, STM image (20×20 nm^2) of a molecular island on Au(111) after deposition at low evaporator temperatures of 550 K prior to being activated. The inset shows the corresponding chemical structure. **d**, STM image (41×41 nm^2) for deposition at an elevated evaporator temperature of 610 K, causing the activation and connection of the molecules to form networks by method II. **e**, STM image (8.5×8.5 nm^2) of a network of eight molecular building blocks. The left and right arrows indicate molecular legs with and without Br atoms, respectively. The chemical structure of the network is drawn in the inset.

The imaging and characterization of the molecular nanostructures were carried out with an STM, running at 7 K (see Supplementary Information, p. S4). The molecules were deposited onto clean Au(111) surfaces, kept at room temperature during deposition. If the evaporator temperature was 550 K or lower during the deposition of the Br_4TPP molecules, large, highly ordered islands (up to 100 nm in diameter) of intact Br_4TPP molecules in a close-packed structure, minimizing the intermolecular distances, were found as a result of molecular diffusion on the surface (Fig. 1c). The molecules in the outermost rows of the islands typically appear different from the inner part, because they often have only three (of four) Br atoms attached. This observation suggests the dissociation of bromine atoms from a small fraction of the molecules at the Knudsen cell temperature used. However, more than 90% of the molecules remain intact, with all four Br atoms present. The exact number of bromine atoms attached to the TPP molecules were determined by a controlled dissociation of one Br atom after another from the molecular core, with voltage pulses between tip and surface of about 2.2 V (see Supplementary Information, p. S5).

The behaviour of the molecules changes fundamentally if the evaporator temperature is raised to at least 590 K. Although some islands of intact molecules (as in Fig. 1c) can still be observed, most of the molecules become activated, with the loss of several Br atoms in the evaporator (method II). Upon thermal diffusion, these activated molecules react with each other to form intermolecular chemical bonds, thereby building macromolecular nanostructures of various shapes on the surface (Fig. 1d). Each molecule provides up to four possible connections to other molecules, resulting in two-dimensional patterns of a different number n of bound molecules (an octamer, $n = 8$, is shown in Fig. 1e). Chains are the preferred shape, as the formation of two-dimensional networks requires more than two connection points between the molecular building blocks. Because of the reduced mobility and diffusion of connected building blocks, the growth is self-limiting and the number of networks on the surface decreases with increasing n. Interestingly, network formation was observed even at a sample temperature of 150 K during evaporation, indicating sufficient diffusion. Note that some of the molecular building blocks have all legs activated, whereas others still have inactive legs with Br atoms attached (Fig. 1e).

In order to show the ability to control the nano-architecture of the macromolecular structures, we synthesized different TPP-based molecules with one, two or four Br substituents (Fig. 2). All molecules are found intact on the surface (in clusters and ordered islands) if low evaporator temperatures are used, and their different structures are reflected in the respective STM intensity distributions (Fig. 2d–f). In the case of sufficient heating, the molecules become activated and connect on the surface, and characteristic molecular arrays are found on the surface. The topology of these nanostructures precisely corresponds to the molecular design (Fig. 2g–o). If only one Br substituent is used (BrTPP), it is exclusively dimers and no larger macromolecular structures that are observed, because each building block provides only one reactive site. Accordingly, the design of porphyrin building blocks with two Br atoms in a linear, that is, *trans* geometry (*trans*-Br_2TPP) leads to the formation of long, linear chains (middle column of Fig. 2). Note that abrupt curvatures (marked by an arrow in Fig. 2h) are

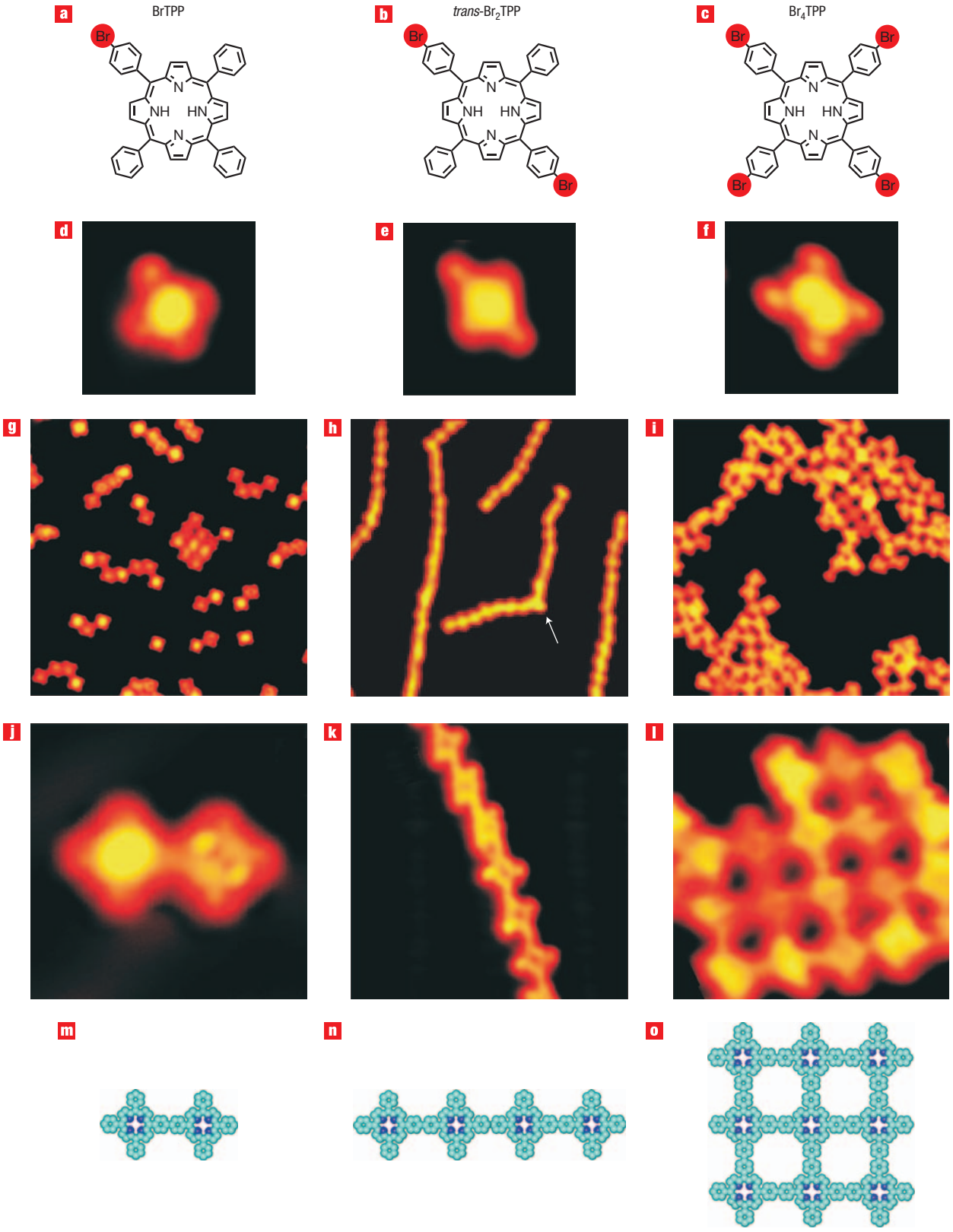

Figure 2 Controlling the macromolecular architecture. Results of different monomer building blocks with one (left column; prepared by method II), two (middle column; method I) and four (right column; method I) Br substituents. **a**–**c**, Chemical structures. **d**–**f**, STM images of single intact molecules (all 3.5 × 3.5 nm^2), where the brominated legs appear larger. **g**–**i**, Overview STM images (all 30 × 30 nm^2) of the nanostructures after activation and connection. In **h**, the arrow indicates where the two linear chains are held together with a weak non-covalent, rather than covalent interaction. **j**–**l**, Detailed STM images of the nanostructures formed (**j**, 5 × 5 nm^2, **k**, 10 × 10 nm^2 and **l**, 8.5 × 8.5 nm^2). **m**–**o**, Corresponding chemical structures of the nanostructures.

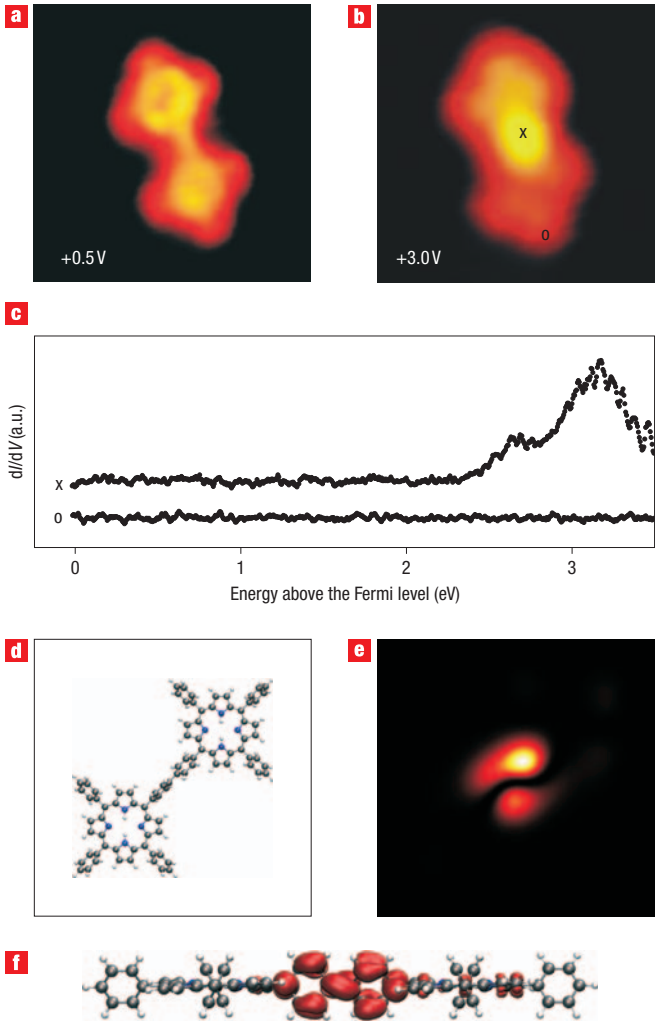

Figure 3 Signature of the covalent character of the intermolecular bonds. STM images (5×5 nm^2) of a porphyrin dimer at sample bias voltages of 0.5 V (**a**) and 3.0 V (**b**) reveal a difference in the electronic structure. **c**, Experimental dI/dV curves. The upper curve (marked by a cross) is obtained at the connection between two molecular units and the lower curve (marked by a circle) is obtained above a bare leg (the two positions are indicated in **b**). **d**, Calculated geometric structure of the isolated dimer. The calculated contribution to the local density of states due to the state at about 2.8 eV above the HOMO is shown in **e** at a vertical distance of 7 Å from the porphyrin plane (that is, a typical tip–surface distance). The same area, 3.5×3.5 nm^2, is examined in **d** and **e**. **f**, Side view of a three-dimensional contour plot of the orbital density of this state at a much higher density.

caused by the attachment of two chains upon weak interaction (as described below). Finally (right column of Fig. 2), the use of four Br substituents at all phenyl legs (Br_4TPP) enables the construction of two-dimensional networks (see also Fig. 1d,e). Accordingly, no macromolecular structures can be formed if TPP molecules without Br substituents are used (see Supplementary Information, p. S7). Therefore, these results clearly show that the architecture of the nanostructures can be precisely controlled through the position of active end groups in the chemical structure of the molecular building blocks. For both methods of activation, only very few Br atoms were found on the surface, which is probably due to desorption during sample heating (method I) and sublimation from the Knudsen cell prior to deposition (method II), respectively.

The intermolecular bonds turn out to be relatively strong compared to bonds within the molecular islands, causing the entire molecular nanostructures (dimers, chains and networks) to follow the pathway of the tip without fragmentation upon pulling on one end with the STM tip (see Supplementary Information, p. S6), whereas the molecules in the islands can be separated easily. Hydrogen bonds, metal–ligand interaction and $\pi-\pi$ stacking can be excluded due to the chemical structure and adsorption geometry of the molecules. The molecules in the networks are therefore likely to be bound covalently through their activated legs as shown schematically in Fig. 1e (note that linkage occurs through the *para* position of the *meso*-phenyl substituents, revealing high selectivity). We want to emphasize that the formation of the networks is not a self-assembly process, because it is not reversible[5].

A signature of the covalent nature of the intermolecular bonds is revealed from spectroscopy measurements and density functional theory (DFT) calculations. The appearance of the nanostructures in the STM images changes fundamentally upon an increase of the bias voltage. While at low voltages the dimer in Fig. 3a appears with homogeneous contrast, an intense protrusion is visible at the connection between the two porphyrin molecules when the voltage is raised to 3 V, but the intensity of the porphyrin cores remains almost unchanged (Fig. 3b). After taking such an image (or dI/dV curves) the integrity of the molecule was controlled by scanning at low voltages. Scanning tunnelling spectroscopy data (Fig. 3c) show that this protrusion is associated with a broad peak around 3 eV, centred around the intermolecular connection, which is absent on the bare leg. These observations suggest the presence of localized orbitals at the connection as supported by DFT calculations (see Supplementary Information, p. S4), using the plane-wave and projector-augmented-wave based code, VASP[20], of an isolated, covalently bound dimer of porphyrin molecules. The experimentally determined distance between two neighbouring porphyrin cores in a nanostructure (17.2 ± 0.3 Å) is in agreement with the calculated distance (17.1 Å) for the relaxed structure shown in Fig. 3d, and so is consistent with the formation of a covalent bond. DFT calculations show that the covalent bond is formed between the two neighbouring phenyl legs, with corresponding C-C bonding (σ) and anti-bonding (σ^*) orbitals. Furthermore, the C-C bonding results in a strong interaction between the two unoccupied, anti-bonding π-orbitals on these two legs, forming in-phase and out-of-phase combinations split by 1.3 eV. The in-phase combination gives rise to an enhancement in the calculated orbital density on the connection between the porphyrin molecules (Fig. 3e,f) about 2.8 eV above the highest occupied molecular orbital (HOMO) level. This energy can be compared with the experimental value of 3 eV for the peak in the tunnelling spectra, because calculations for a TPP molecule adsorbed on a Au(111) surface show that the molecule is weakly adsorbed and that the HOMO level is nearly aligned with the Fermi level (see Supplementary Information, p. S4). The protrusion seen in the STM images and the peak in the spectroscopy data at biases of around 3 V can be rationalized by the increased local density of states above the connection due to this particular electronic state. Note that this characteristic signature of the covalent bond is observed for all nanostructures.

Connection of the building blocks always takes place on the surface, because the sublimation of dimers or networks, if they were formed in the Knudsen cell using method II, would require higher evaporator temperatures. Furthermore, dimers (and certainly networks) are expected to decompose at these

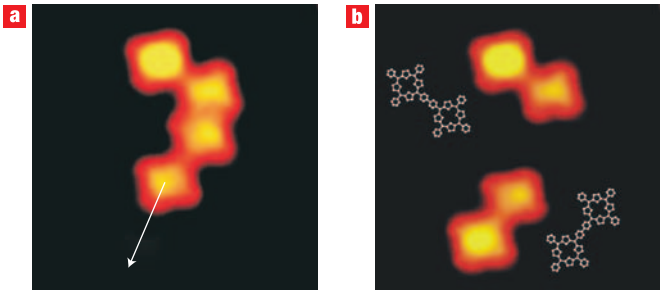

Figure 4 Weak and strong intermolecular forces in lateral manipulation. **a**,**b**, STM images (9×9 nm^2) before (**a**) and after (**b**) lateral manipulation by the tip along the pathway indicated by an arrow in **a**, leading to the separation of the two porphyrin dimers.

temperatures in the Knudsen cell[21]. Formation in the gas phase can be excluded due to the low molecular density. By using both methods for all studied molecular building blocks, we found method I to be more efficient than II, probably because of the enhanced diffusion. On the other hand, this diffusion upon sample heating leads to enhanced clustering of the networks created (Fig. 2i) compared with the sample kept at room temperature (Fig. 1d).

In a next step, complex network architectures could be constructed by selective activation of different molecular sites at characteristic dissociation temperatures (using method I). We want to emphasize that the availability of two complementary techniques (I and II) can be of great advantage, in particular if the molecular weight does not allow activation and evaporation at the same time. Furthermore, method II can be of great importance in preparing more sophisticated surface structures where sample heating must be avoided due to previous preparation of films or (for example, self-assembled) nanostructures on the surface.

As is visible in Fig. 2g, the dimers on the surface accumulate in clusters (or large islands, see Supplementary Information, p. S8), where they indent each other by minimizing the distance between them (similar clustering is also observed for chains and networks). The relative strength of the covalent bond within a dimer and the weak interaction between two dimers is demonstrated by lateral manipulation (Fig. 4). When pulling the end of a dimer with the STM tip, only the manipulated dimer follows and remains intact, and the other dimer does not change its position on the surface. This result demonstrates the different intermolecular forces within a dimer and between dimers: covalent versus non-covalent interactions.

As a consequence, the formed covalently bound nanostructures could in principle be capable of charge transport between the molecular building blocks. Furthermore, the porphyrin core can act as a platform for further construction of highly functional nanostructures by coordination of electronically, optically or magnetically active ions[22]. These results pave the way to bottom-up assembly of stable nano-architectures with possible future applications in molecular electronics and sensing devices.

Received 24 July 2007; accepted 28 September 2007;
published 28 October 2007.

References

1. Joachim, C., Gimzewski, J. K. & Aviram, A. Electronics using hybrid-molecular and mono-molecular devices. *Nature* **408,** 541–548 (2000).
2. Heath, J. R. & Ratner, M. A. Molecular electronics. *Physics Today* **56,** 43–49 (2003).
3. Nitzan, A. & Ratner, M. A. Electron transport in molecular wire junctions. *Science* **300,** 1384–1389 (2003).
4. Cote, A. P. *et al.* Porous, crystalline, covalent organic frameworks. *Science* **310,** 1166–1170 (2005).
5. Whitesides, G. M. & Grzybowski, B. Self-assembly at all scales. *Science* **295,** 2418–2421 (2002).
6. Theobald, J. A., Oxtoby, N. S., Phillips, M. A., Champness, N. R. & Beton, P. H. Controlling molecular deposition and layer structure with supramolecular surface assemblies. *Nature* **424,** 1029–1031 (2003).
7. Barth, J. V., Costantini, G. & Kern, K. Engineering atomic and molecular nanostructures at surfaces. *Nature* **437,** 671–679 (2005).
8. Barth, J. V., Weckesser, J., Lin, N., Dmitriev, A. & Kern, K. Supramolecular architectures and nanostructures at metal surfaces. *Appl. Phys. A* **76,** 645–652 (2003).
9. Pawin, G., Wong, K. L., Kwon, K.-Y. & Bartels, L. A homomolecular porous network at a Cu(111) surface. *Science* **313,** 961–962 (2006).
10. van Hameren, R. *et al.* Macroscopic hierarchical surface patterning of porphyrin trimers via self-assembly and dewetting. *Science* **314,** 1433–1436 (2006).
11. Stöhr, M. *et al.* Controlling molecular assembly in two dimensions: The concentration dependence of thermally induced 2D aggregation of molecules on a metal surface. *Angew. Chem. Int. Edn* **44,** 7394–7398 (2005).
12. Keeling, D. L. *et al.* Assembly and processing of hydrogen bond induced supramolecular nanostructures. *Nano Lett.* **3,** 9–12 (2003).
13. Yokoyama, T., Yokoyama, S., Kamikado, T., Okuno, Y. & Mashiko, S. Selective assembly on a surface of supramolecular aggregates with controlled size and shape. *Nature* **413,** 619–621 (2001).
14. Rabe, J. P. & Buchholz, S. Commensurability and mobility in two-dimensional molecular patterns on graphite. *Science* **253,** 424–427 (1991).
15. Lin, N., Dmitriev, A., Weckesser, J., Barth, J. V. & Kern, K. Real-time single-molecule imaging of the formation and dynamics of coordination compounds. *Angew. Chem. Int. Edn* **41,** 4779–4783 (2002).
16. Hla, S. W., Bartels, L., Meyer, G. & Rieder, K.-H. Inducing all steps of a chemical reaction with the scanning tunneling microscope tip: towards single molecule engineering. *Phys. Rev. Lett.* **85,** 2777–2780 (2000).
17. Hla, S.-W., Meyer, G. & Rieder, K.-H. Selective bond breaking of single iodobenzene molecules with a scanning tunneling microscope tip. *Chem. Phys. Lett.* **370,** 431–436 (2003).
18. Spillmann, H. *et al.* A two-dimensional porphyrin-based porous network featuring communicating cavities for the templated complexation of fullerenes. *Adv. Mater.* **18,** 275–279 (2006).
19. Iancu, V., Deshpande, A. & Hla, S.-W. Manipulation of the Kondo effect via two-dimensional molecular assembly. *Phys. Rev. Lett.* **97,** 266603 (2006).
20. Kresse, G. & Furthmüller, J. Efficient iterative schemes for *ab initio* total-energy calculations using a plane-wave basis set. *Phys. Rev. B* **54,** 11169–11186 (1996).
21. Zambelli, T. *et al.* Deposition of large organic molecules in ultra-high vacuum: A comparison between thermal sublimation and pulse-injection. *Int. J. Nanosci.* **3,** 331–341 (2004).
22. Gottfried, J. M., Flechtner, K., Kretschmann, A., Lukasczyk, T. & Steinrück, H.-P. Direct synthesis of a metalloporphyrin complex on a surface. *J. Am. Chem. Soc.* **128,** 5644–5645 (2006).

Acknowledgements

We thank F. Moresco for discussions. This work was supported by the Deutsche Forschungsgemeinschaft (DFG) through contract no. GR 2697/1-1 and by the European Union through the Integrated Project PICO INSIDE and the Marie-Curie Research Training Network PRAIRIES, contract MRTN-CT-2006-035810. M.P. is grateful for support from the Humboldt foundation and the Swedish Research Council (VR).
Correspondence and requests for materials should be addressed to L.G.
Supplementary information accompanies this paper on www.nature.com/naturenanotechnology.

Author contributions

L.G. and S.H. conceived the experiments. L.G. performed the experiments (partly with L.L.) and analysed the data. M.D. and M.P. were in charge of the calculations. M.V.P. and S.H. synthesized the molecules. L.G. wrote the paper. L.G., M.D., M.P. and S.H. discussed the results and commented on the manuscript.